CERN EP-ADP-OS

A study of the sensitivity to the top quark mass of the top-antitop invariant mass distribution measured at $\sqrt{s} = 8$ TeV with the ATLAS detector

Varsiha Sothilingam

Supervisors: Alexis Vallier, Stefano Camarda

Abstract

The sensitivity of the top quark mass of the invariant-mass distribution to top quark pairs produced in proton proton collisions is investigated with a blinded analysis. The study is based on the normalised differential cross section as a function of the top-antitop invariant-mass measured at $\sqrt{s} = 8$ TeV with the ATLAS detector in the semileptonic decay channel and corresponding to an integrated luminosity of 20.3 fb^{-1}. The analysis is performed at next-to-leading and next-to-next-to-leading orders in the perturbative expansion of the strong-coupling constant. The estimated total uncertainty on the top mass is $^{+0.5}_{-0.7}$ GeV.

Geneva, Switzerland

September 10, 2019

1 Introduction

The top quark is the heaviest elementary particle known to date, and the only quark whose mass resides at the electroweak symmetry breaking scale. It is the only fermion whose Yukawa coupling to the Higgs boson is of the order of unity. Among the properties of the top quark, its mass plays a crucial role in the study of the quantum vacuum stability [1], and in the fit of the parameters of the electroweak sector in the Standard Model [2].

The most precise measurements of the top quark exploit the sensitivity of kinematic properties of its decay products, and aim at fully reconstructing the top quark. These methods, which are referred to as direct measurements, rely on general purpose event generators, which include parton showering and hadronisation models. There is a debate whether they yield a measurement of the top quark mass in the pole-mass renormalisation scheme [3], or whether there is an additional ambiguity in the interpretation of these top quark mass measurements as such Ref. [4].

Alternative measurements, which exploit the sensitivity of cross section, rely on perturbative QCD predictions and allows one to determine the mass of the top quark in a well-defined renormalisation scheme. These measurements are less precise, but more unambigously related to the top quark pole mass. They provide invaluable insight into the issue of relating direct measurements of top quark mass to the pole mass.

The world average of the top quark mass from direct measurement is 172.9 ± 0.4 GeV, whereas for the pole mass from cross-section measurement, it is 173.1 ± 0.9 GeV [5]. These values are averages of the mass values measured by the CDF, D0, CMS, and ATLAS experiments.

The invariant mass distribution of a top-antitop pair produced in hadron collisions is sensitive to the top quark mass, and can be used to measure this parameter in the pole-mass scheme, by using perturbative QCD predictions. Figure 1 shows the differential cross section as a function of the invariant mass of the top-antitop pair, $m_{t\bar{t}}$, for various different values of the top mass, m_t. The cross section is nonzero only above the phase-space threshold of twice m_t, and in the proximity of this threshold the cross section is proportional to the velocity of the top quark.

The data used for this study are $t\bar{t}$ events at a centre-of-mass energy of 8 TeV collected by ATLAS. This study focuses on normalised cross section in order to avoid large theoretical uncertainties on the total cross section due to missing higher orders in perturbative QCD. Moreover the use of normalised cross section avoids correlation of theoretical uncertainty with m_t determination from total cross section measurements and allows combination with the latter.

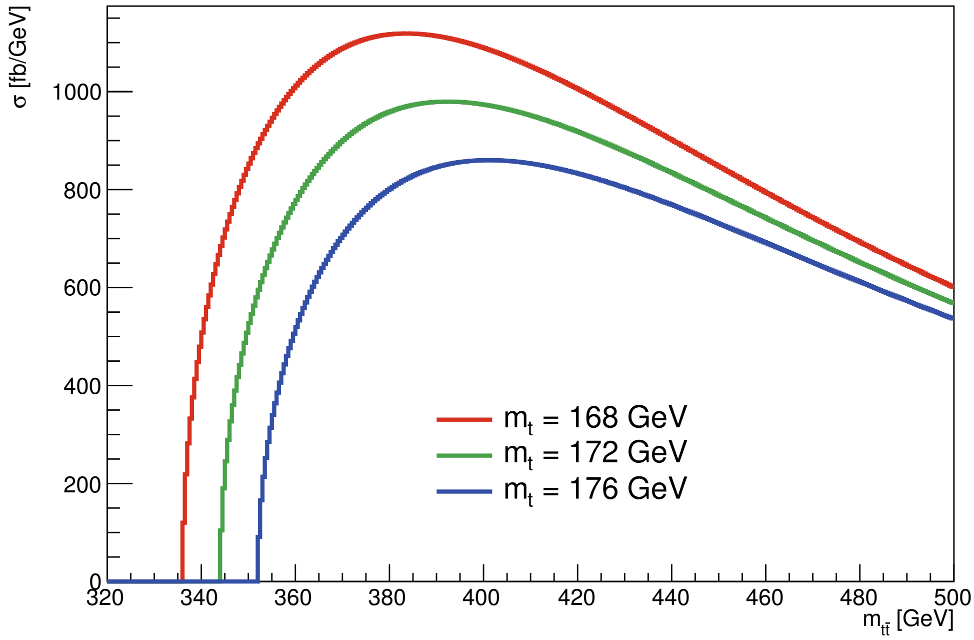

Figure 1: Top pair production cross section as a function of $m_{t\bar{t}}$ in the threshold region for varying mass points in the range 320 GeV to 500 GeV. Predictions are evaluated at leading order.

2 Methodology

The study is based on the ATLAS measurement of differential cross sections as a function of $m_{t\bar{t}}$, corresponding to an integrated luminosity of 20.3 fb^{-1} and measured in the lepton + jets decay channel [6]. The invariant mass of the $t\bar{t}$ system is poorly reconstructed due to the presence of a neutrino in the final state. The neutrinos transverse momentum is inferred indirectly from momentum balance in the transverse plane and its longitudinal momentum is not measured.

Top-antitop production in hadron collisions at leading order are proportional to α_S^2. Theory predictions are evaluated at next-to-leading-order (NLO), that are $\mathcal{O}(\alpha_S^3)$, using `MCFM` [7], whereas next-to-next-to-leading-order (NNLO) predictions, that are $\mathcal{O}(\alpha_S^4)$, are taken from Ref.[6]. The `MCFM` programme, "Monte Carlo for FeMtobarn processes" calculates partonic cross sections for femtobarn level processes, at hadron colliders . The NLO `MCFM` predictions are interfaced to `applGRID` [8] for the fast convolution with parton distribution functions (PDF) and for the fast evaluation of QCD scale variations. The NNLO predictions are interfaced to `fastNLO`. The `fastNLO` tables are taken from Ref.[6] which uses a reference mass of m_t= 173.3 GeV. The `applGRID` tables are created for a range of masses from 168 to 178 GeV.

There are three main steps in `applGRID` producing theory predictions, grids, at NLO. The first step consists in producing vegas preconditioning grids. The vegas algorithm is a type of Monte Carlo integration that is based on importance sampling. It uses probability distribution of the integrand function to concentrate the sampling points into the region with the largest probability [9]. The second step is a phase space sampling which produces a preliminary grid used to determine the x and Q^2 ranges of each bin of the $m_{t\bar{t}}$ distribution. The final step releases the PDF convolution on the phase space defined by the previous step. The second and third steps were parallelised to improve the numerical accuracy of the predictions on the HTCondor system available at CERN.

The χ^2 evaluation and minimisation are performed using the software xFitter-an open-source project for the determination of PDFs [10]. The measured cross section is compared to the theory predictions by means of a χ^2 probability test. The minimum of the χ^2 as a function of m_t yields the measurement of the top quark mass. Its half width at one unit above the minimum provides an estimate of the associated uncertainty. The χ^2 is defined as $\chi^2 = \sum_{ij}(m_i - \mu_i)^{\mathrm{T}} V^{-1}(m_i - \mu_j)$ where m_i is the measured normalised cross section in bin i, μ_i is the corresponding theory prediction and V is the covariance matrix. The systematic uncertainties are included in the χ^2 with a formulation mathematically equivalent to nuisance parameters for profiled likelihood analysis.

Figure 2 shows NLO predictions of the normalised cross section as a function of $m_{t\bar{t}}$ distribution in the bins, corresponding to the ATLAS measurement for varying mass points 168, 172 and 178 GeV, and illustrates the sensitivity to the top quark mass. The up and down variations of the top mass are asymmetric. The asymmetry is likely to be due to the fact that the lowest edge of the first bin is 345 GeV. Hence when m_t is lower than 172.5 GeV the lowest bin edge is higher than the phase-space threshold equal to $2 \cdot m_t$, and part of the cross section ends up in the underflow bin.

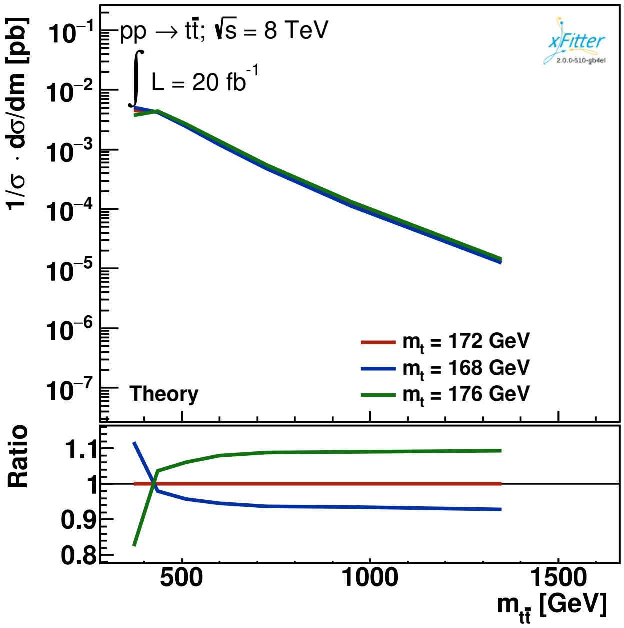

Figure 2: Normalised differential cross section against $m_{t\bar{t}}$ for three reference top quark mass points of 168, 172 and 176 GeV.

3 Physics modelling

Predictions are computed at NLO for different top quark mass in the range 168 to 178 GeV. At each value of the top quark mass, the NLO predictions are corrected to NNLO using the ratio of NNLO to NLO predictions at the reference mass of m_t = 173.3 GeV.

This study uses the CT14NNLO PDF set and $\alpha_S = 0.118$. The PDF uncertainties are scaled from 90% to 68% confidence level and α_S is varied in the range $\pm$ 0.001. The missing predictions at higher order uncertainties are estimated through variations of the renormalisation and factorisation scales. Each scale is varied independently by factors of 2 and 0.5, and the corresponding cross section variations are added in quadrature. The QCD scale variations are evaluated at NLO. Since the predictions are corrected to NNLO, they yield a conservative estimate of the missing higher-order uncertainty. The PDF uncertainties and scale variations are included in the χ^2 as nuisance parameters.

Figure 3 shows NLO predictions at the reference mass of m_t = 173.3 GeV, including the PDF uncertainties and QCD scale variations and the total uncertainty-which is the quadratic sum of the two.

Figure 4 shows a comparison of `applGRID` predictions at m_t = 173.3 GeV

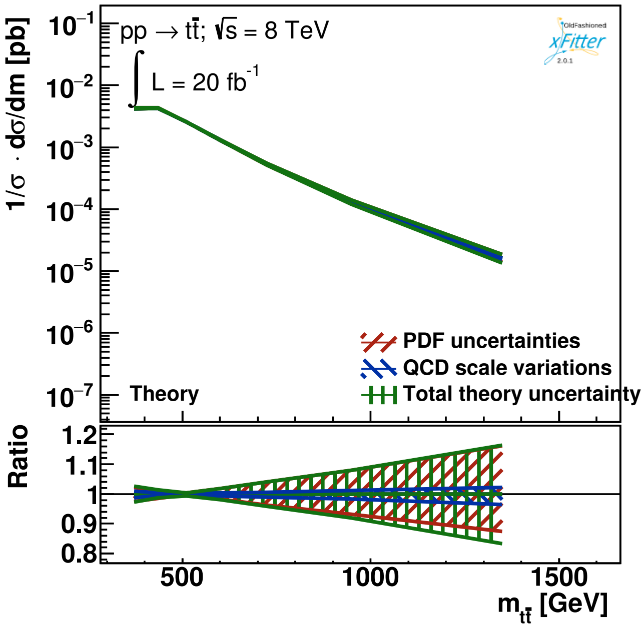

Figure 3: Normalised differential cross section as a function of $m_{t\bar{t}}$ showing PDF uncertainties including α_S variations and QCD scale variations.

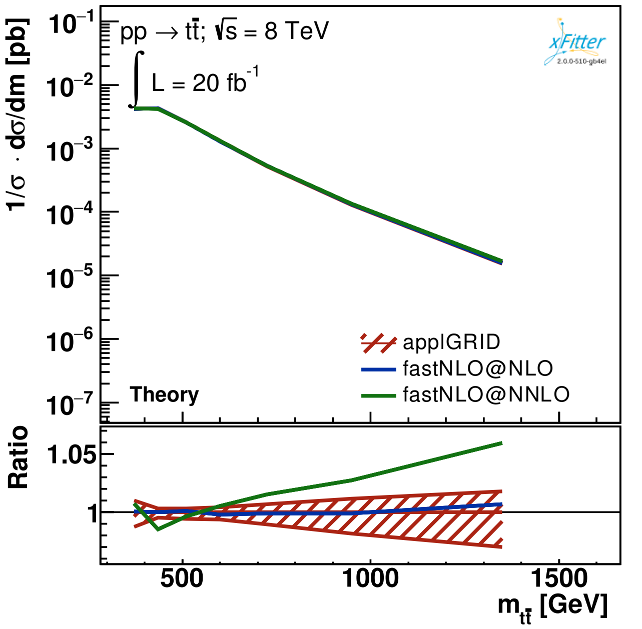

Figure 4: Comparison of `applGRID` and `fastNLO` grids

with the `fastNLO` grids both at NLO and NNLO. This plot provides a benchmark of the two methods for creating the grids and exposes the key differences in the theory between NLO and NNLO. One can see that `fastNLO` at NLO is consistent with `applGRID`. On the contrary NNLO predictions are not consistent with NLO predictions, within the scale variation bands. This indicates that the α_s^4 corrections are significant and should be accounted for.

4 Correlation model for the experimental uncertainties

The measured differential cross section as a function of $m_{t\bar{t}}$ [6] used in this study is affected by various sources of uncertainties. They comprise the statistical uncertainty, and several sources of systematic uncertainty. The statistical uncertainty quoted for the normalised $m_{t\bar{t}}$ distribution in Ref.[6] does not include any bin-to-bin correlation. However a certain amount of (anti)correlation exists due to the normalisation procedure. In order to estimate the bin-to-bin statistical correlation of the normalised cross section, one can apply standard error propagation to the statistical uncertainty of the normalised differential cross section.

The bin width for which we are looking at the data is defined to be W_i, for the corresponding i^{th} bin. Measured differential cross section for the i^{th} bin is defined as $\partial\sigma^i_{t\bar{t}}$. Integrating over each bin one obtains the normalised cross section:

$$\sigma^i_{t\bar{t}} = W_i \cdot \partial\sigma^i_{t\bar{t}} \tag{1}$$

Taking the sum one obtains the total cross section for $t\bar{t}$ events:

$$\sum_i \sigma^i_{t\bar{t}} = \sum_i W_i \partial\sigma^i_{t\bar{t}} = \sigma^{total}_{t\bar{t}}. \tag{2}$$

The bin-integrated normalised cross sections for i^{th} bin ($\varsigma^i_{t\bar{t}}$) is defined by the ratio between the normalised cross section in bin i (Eqn 1) and the total cross section (Eqn 2):

$$\varsigma^i_{t\bar{t}} = \frac{\partial\sigma^i}{\sigma^{t\bar{t}}_{total}} = \frac{W_i \partial\sigma^i_{t\bar{t}}}{\sum_j \sigma^j_{t\bar{t}}} \tag{3}$$

$\varsigma^i_{t\bar{t}}$ for different bins are statistically correlated unlike $\sigma^i_{t\bar{t}}$. The covariance matrix for the normalised uncertainties of $\varsigma^i_{t\bar{t}}$ is V where:

$$\mathbf{V} = \mathbf{G}\mathbf{S}\mathbf{G}^{\mathbf{T}} \tag{4}$$

S is the diagonal covariance matrix of the uncertainties s_i measured on $\sigma^i_{t\bar{t}}$. The diagonal elements are s_i^2 and off diagonal elements are trivially zero.
G is the matrix of partial derivatives $\mathbf{G}_{ij}$ where:

$$\mathbf{G}_{ij} = \frac{\delta_{ij}}{\sigma^{t\bar{t}}_{total}} - \frac{\sigma^i_{t\bar{t}}}{{\sigma^{t\bar{t}}_{total}}^2} \tag{5}$$

This method of calculating the statistical uncertainties can be used to calculate the systematic uncertainties on normalised cross section as well. The systematic uncertainties derived with this method have been compared provided by Ref. [6] and they were found to be in good agreement.

In calculating the normalised statistical covariance matrix for the normalised differential cross sections, one obtains the following correlation plot, ρ_{ij}, figure 5. The largest correlation is -44%. It is negative as the number of events over all bins must be constant. Therefore the increase in events for bin i will lead to a decrease in events for bin j. It is the case for all correlation values ρ_{ij} where $i \neq j$, as seen in the plot.

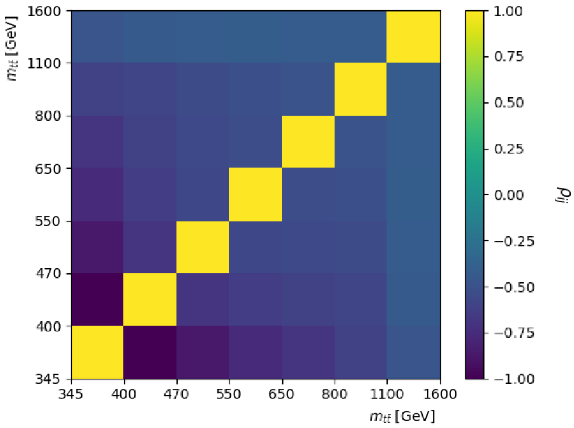

Figure 5: Statistical correlation matrix for normalised cross sections [6].

5 Closure test

As the first step of the analysis we perform a closure test for which we use the theory prediction of the $m_{t\bar{t}}$ distribution at m_t = 173.3 GeV as pseudo-data. The m_t value is extracted and compared to the input value. This simple test already provides a realistic estimate of the experimental and theoretical uncertainties. The result of the closure test are shown in figure 6 using the original statistical uncertainty provided by Ref [6]. The extracted value of m_t is 173.18 GeV, which agrees within 0.12 GeV with the input value. The estimated total uncertainty found was $\pm$ 0.6 GeV.

Figure 7 shows results corresponding to a closure test in which the correlation matrix of the statistical uncertainties derived in Section 4 is used. Similar uncertainties are observed, with a relative increase of 5% in the statistical uncertainty and a relative decrease of 20% in systematic uncertainties.

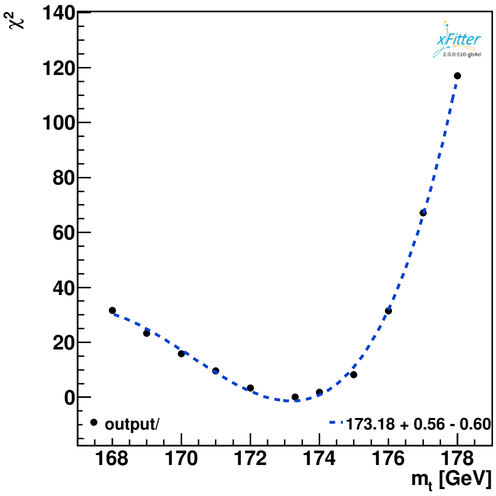

(a) χ^2 scan

	output
$m_t[GeV]$	173.18
Statistical	$+0.21 - 0.20$
Systematic	$+0.37 - 0.37$
PDFs	$+0.26 - 0.26$
QCD scales	$+0.15 - 0.15$
Total (decomposed)	$+0.52 - 0.52$
Total (from fit)	$+0.56 - 0.60$

(b) Output mass and uncertainties

Figure 6: $\chi^2(m_t = 173.3\text{ GeV})$ for normalised differential cross sections

6 Blinding of data test

The blinding of data is completed by shifting the reference mass used to create the theory prediction, grids. It is done to avoid bias when performing analysis. The method of blinding was done by adding a shift to the reference value $m_{ref} + \Delta$ where Δ is a randomly generated shift applied to all the predictions used in the χ^2 scan. This value is in the range [-5, +5] GeV, generated with a uniform distribution.

Figure 8 shows the χ^2 scan for the blinded pseudo-data grids for a prediction reference mass of 173.3 GeV. Looking at the central value found in this scan, it is 171.55 GeV which shows the central value has been shifted by -1.68 GeV,

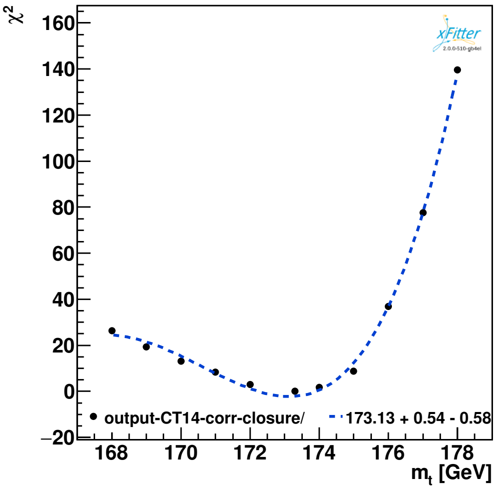

(a) χ^2 scan

	output
$m_t[GeV]$	173.13
Statistical	$+0.22-0.21$
Systematic	$+0.30-0.31$
PDFs	$+0.25-0.25$
QCD scales	$+0.14-0.14$
Total (decomposed)	$+0.47-0.47$
Total (from fit)	$+0.54-0.58$

(b) Output mass and uncertainties

Figure 7: $\chi^2(m_t = 173.3 \text{ GeV})$ for normalised differential cross sections

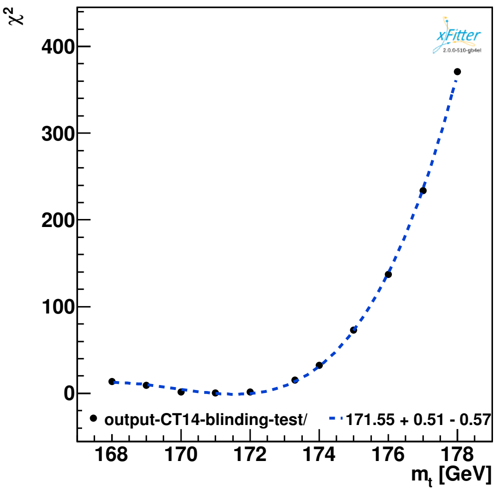

(a) χ^2 scan

	output
$m_t[GeV]$	171.55
Statistical	$+0.23-0.23$
Systematic	$+0.27-0.28$
PDFs	$+0.25-0.25$
QCD scales	$+0.15-0.15$
Total (decomposed)	$+0.46-0.47$
Total (from fit)	$+0.51-0.57$

(b) Output mass and uncertainties

Figure 8: $\chi^2(m_t = 173.3+\Delta)$ GeV for normalised differential cross sections

from 173.3 GeV. If the predicted mass is below the unblinded reference mass, Δ is postive, and vice versa. This is because all the grid files have been shifted in the direction of the shift and so the predicted value will shift in the opposite direction. When unblinding the data and revealing the shift value, one will find it to be +1.96469 GeV. With the inclusion of the uncertainties, the shift value is consistent with the values observed, successfully blinding the data.

7 Results and Conclusion

Performing the analysis on the real blinded data both at NLO and NNLO allows one to observe the NNLO correction to NLO predicted top quark mass. The blinding used here is different to that in the blinding test performed on psuedo-data.

With the χ^2 scan at NLO, it was with the inclusion of both PDF with α_S and QCD scale variations, as seen in the results below. At NNLO the scale variations are never applied as they have not been normalised at NNLO.

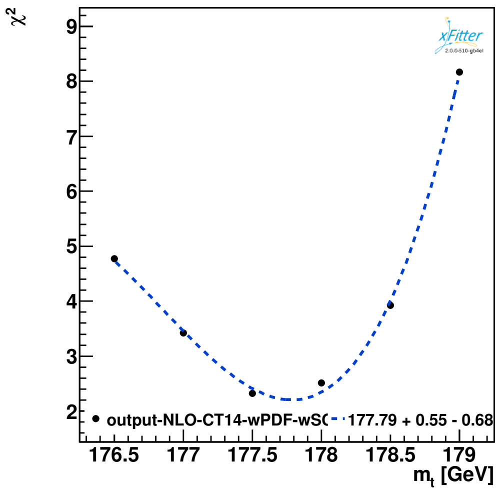

(a) χ^2 scan

χ^2 at minimum	2.2
m_t [GeV]	177.79
Statistical	$+0.30-0.32$
Systematic	$+0.37-0.41$
PDFs	$+0.31-0.33$
QCD scales	$+0.19-0.20$
Total (decomposed)	$+0.60-0.65$
Total (from fit)	$+0.55-0.68$

(b) Output χ^2 and mass with uncertainties

Figure 9: χ^2 and m_t for NLO calculations with uncertainty decomposition including both PDF and QCD scale variations.

The main result from this analysis and the central value of the top quark mass for which the χ^2 minimisation was found to be m_t = 177.79 GeV. The NNLO correction to the uncertainty of the top mass, $\Delta m_t^{\rm NNLO}$, is calculated by the mass shift between this result and NNLO with PDF uncertainties. The mass shift found was $\Delta m_t^{\rm NNLO}$= 0.179 GeV giving a final result of m_t = 177.79 $\pm$ 0.179 GeV. Shift is comparable with the estimate of missing higher order uncertainties at NLO performed with QCD scale variations. For the results, the difference in the χ^2 = 0.5- the NNLO correction to the χ^2 value. As expected the NNLO study reduces the χ^2 value.

The normalised differential cross section as a function of the top-antitop invariant-mass measured by ATLAS at $\sqrt{s} = 8$ TeV was used to perform a sensitivity study for the measurement of the top quark mass with a blinded analysis. The correlation of statistical uncertainty was estimated by error propagation. The analysis was performed at NLO and NNLO, yielding a total uncertainty is $^{+0.5}_{-0.7}$ GeV, illustrating that this data has the potential for a measurement of the top quark pole mass competitive to the world average. At this level of accuracy further corrections, such as those arising from bound state corrections and NLO electroweak calculations must be considered as they are expected to be of the same order of the total estimated uncertainty.

References

[1] G. Degrassi et al., Higgs mass and vacuum stability in the Standard Model at NNLO, JHEP 1208 (2012) 098, DOI: 10.1007/JHEP08(2012)098

[2] J. Haller et al., Update of the global electroweak ft and constraints on two-Higgs-doublet models, Eur. Phys. J. C 78 (2018) 8, 675, DOI: 10.1140/epjc/s10052-018-6131-3

[3] P Nason et al., The Top Mass in Hadronic Collisions, arXiv:1712.02796v3

[4] B. Dehnadi, A. H. Hoang, V. Mateu, M. Preisser and I. W. Stewart, Monte Carlo Top Quark Mass Calibration, PoS RADCOR **2017** (2018) 062 doi:10.22323/1.290.0062 [arXiv:1803.02321 [hep-ph]].

[5] Particle Data Group 2019,M. Tanabashi et al. (Particle Data Group), Phys. Rev. D 98, 030001 (2018)

[6] The ATLAS Collabaration, Measurements of top-quark pair differential cross-sections in the lepton+jets channel in pp collisions at $\sqrt{s} = 8$ TeV using the ATLAS detector, arXiv:1511.04716

[7] J. M. Campbell, R. K. Ellis, W. Giele, T. Neumann, C. Williams, MCFM v8.3 Users Guide, mcfm.fnal.gov/mcfm.pdf

[8] Carli, T., Clements, D., Cooper-Sarkar, A. et al. A posteriori inclusion of parton density functions in NLO QCD final-state calculations at hadron colliders: the APPLGRID project, Eur. Phys. J. C (2010) 66: 503, DOI: 10.1140/epjc/s10052-010-1255-0

[9] GNU.org, Monte Carlo Integration, Monte Carlo Integration- GSL 2.6 Documentation

[10] V. Bertone *et al.* [xFitter Developers' Team], PoS DIS **2017** (2018) 203 doi:10.22323/1.297.0203 [arXiv:1709.01151 [hep-ph]].